European Journal of Control xxx (xxxx) xxx

Contents lists available at ScienceDirect

European Journal of Control

journal homepage: www.elsevier.com/locate/ejcon

Robust observer design with prescribed settling-time bound and finite varying gains☆,☆☆

Ramón I. Verdés Kairuz[a], Yury Orlov[b,*], Luis T. Aguilar[a]

[a] Instituto Politécnico Nacional—CITEDI, Avenida Instituto Politécnico Nacional 1310 Colonia Nueva Tijuana, Tijuana 22435, Baja California, México
[b] Department of Electronics and Telecomunications, Mexican Scientific and Advanced Studies Center of Ensenada, Carretera Ensenada-Tijuana No. 3918, Zona Playitas, Ensenada 22860, Baja California, México

ARTICLE INFO

Article history:
Received 4 April 2022
Accepted 5 June 2022
Available online xxx

Recommended by Prof. T Parisini

Keywords:
Prescribed-time observer
State estimation
Sliding mode

ABSTRACT

Robust observer design is developed for a normal form system with a prescribed upper bound on the observer convergence time irrespective of initial state values and matched uniformly bounded disturbances. The design recasts a finite-time observer, especially developed for a system composed of diagonal and over-diagonal forms, and it is based on the scaling technique. The proposed observer operates with time-varying gains, uniformly bounded on an infinite horizon, thereby yielding an attractive implementation opportunity compared to the original design by Holloway and Krstic [6] with time-varying gains, which escape to infinity as time goes to the prescribed time instant. Capabilities of the present observer are supported in a numerical study, performed for a perturbed triple integrator, and are compared to existing prescribed-time and fixed-time observers.

1. Introduction

High-gain observers are long-recognized for their robustness, and they are therefore widely used in output feedback to recover frequency-domain loop properties achieved by state feedback [8]. Although the peaking phenomenon, which is typical for such observers, may potentially induce finite escape time while interacting with nonlinearities, its duration is however very short compared to the time scale of the plant variables because the observer dynamics are much faster than the closed-loop dynamics. Hence, the closed-loop trajectories remain near their initial values during the observer peaking period that adds practical value to the use of high-gain observers in nonlinear output feedback.

Recently, the time-varying high-gain observers of linear systems in the canonical observability form and their use in output feedback design of normal-form linear systems were respectively explored in [6,7] to achieve a prescribed convergence time regardless of initial conditions and certain external disturbances. High-gain scaling technique was then extended in [22] to prescribed-time stabilization of general linear systems and further developed in [9,10,23] to a class of nonlinear (strict feedback) systems with state-dependent uncertainties throughout the system dynamics.

The feedback algorithms, proposed in the above works [6,7,9,10,22,23], collected attractive stability and robustness features at the transition stage, while being confined to the prescribed time interval because of using time-varying gains, escaping to infinity as time approached the prescribed instant T. For non-stop running of strict-feedback-like systems beyond the prescribed convergence time, the extended scaling technique was applied in [21] to states and virtual control inputs, although it suffered from time-varying unlimited gains as well.

To prevent the high gain implementation problem prescribed time stabilizing nonlinear feedback laws were deduced in [1,2,5,15,18,20] for uncertain systems in normal form by recasting their sliding mode finite-time stabilizing counterparts. The present investigation relies on the baseline time scaling of the seminal work [17] and extends the state transformation, proposed in [15] for the double integrator observer design, to arbitrary order systems in normal form.

As in [15], the resulting observer design operates with finite time-varying gains over an infinite horizon and it ensures both attractive robustness features against matched uniformly bounded disturbances and prescribed-time upper bound on the observer convergence, regardless of initial conditions and admissible disturbances. In contrast to the original prescribed-time observer design [6] with time-varying gains, which escape to infinity as time goes to the prescribed time instant, the present design prevents in-

☆ Recommended by: Prof. T Parisini

☆☆ This work was supported by the Mexican Council of Science and Technology (CONACYT) under grants 285279 and A1-S-9270.

* Corresponding author.
E-mail addresses: rverdes@citedi.mx (R.I. Verdés Kairuz), yorlov@cicese.mx (Y. Orlov), laguilarb@ipn.mx (L.T. Aguilar).

https://doi.org/10.1016/j.ejcon.2022.100667
0947-3580/

finitely large gains from being used, thereby admitting its straightforward implementation. The developed observer with such properties forms *the main contribution* of the paper.

It is worth noticing that the dimensionality extension that the present work makes beyond [15] is far from being trivial. It recasts a basic finite-time observer, especially developed for a system, composed of diagonal and over-diagonal forms, unlike that of [15] where the well-known supertwisting observer was straightforwardly recast to its time-varying version, possessing a prescribed-time upper bound on the observer convergence time.

The outline of the rest of the paper is as follows. Section 2 derives a finite-time observer for a generic system, composed of diagonal and over-diagonal forms, from its existing counterpart for normal (over-diagonal) form. Section 3 develops a fixed-time observer for an arbitrary order system in normal form with a prescribed-time upper bound on the observer convergence time. Section 4 illustrates capabilities of the proposed prescribed-time observer for a perturbed triple integrator in comparison with existing prescribed- and fixed-time observers [6] and [12]. Section 5 collects some conclusions.

1.1. Notation and definitions

Throughout the paper, the following notation is used.

- $\mathbb{R}_+ = \{x \in \mathbb{R} : x \geq 0\}$;
- $\lceil z \rfloor^\alpha = |z|^\alpha \operatorname{sign}(z)$, $\alpha \geq 0$, $z \in \mathbb{R}$;
- I_n is the identity matrix of order n.

Solutions of a generic piece-wise continuous system

$$\dot{x} = f(x,t), \quad x(t_0) = x^0 \in \mathbb{R}^n, \tag{1}$$

are viewed in the sense of Filippov [4].

Definition 1 [14]**.** Let a piece-wise continuous system (1) possess an equilibrium in the origin. It is said to be globally finite-time stable if it is globally asymptotically stable, and any solution $x(t,t_0,x^0)$ of (1) resets to zero in some finite time $T(t_0,x^0)$, i.e., $x(t,t_0,x^0) = 0$ for all $t \geq t_0 + T(t_0,x^0)$ where

$$T(t_0,x^0) = \inf\{t \geq 0 : x(\tau,t_0,x^0) = 0 \text{ for all } t \geq t_0 + \tau\} \tag{2}$$

is the settling-time function.

System (1) is additionally said to be *fixed-time stable* provided that its settling-time function is uniformly bounded over the entire domain of initial conditions.

Definition 2 [16]**.** Finite-time stable system (1) is referred to as fixed-time stable if there exists an absolute upper bound $T_{\max}$ of the settling-time function $T(t_0,x^0)$ so that $T(t_0,x^0) \leq T_{\max}$ for all $(t_0,x^0) \in \mathbb{R}^{n+1}$.

A fixed-time stable system, which admits, by means of an appropriate gain tuning, a stabilization at an arbitrarily small time instant, irrespectively of its initial state, is said to be *stabilizable in prescribed-time* [17].

2. Preliminaries: finite-time observer design

The background material is first presented for an observer design of an arbitrary order linear system in canonical form and then it is extended to a particular non-canonical form which is suitable for the subsequent prescribed-time generalization.

2.1. Design for upper-diagonal canonical form

Consider system

$$\dot{\zeta}(s) = \Lambda\zeta(s) + B\Big(u(s) + w(s)\Big),$$
$$y_\zeta(s) = C\zeta(s), \tag{3}$$

in the upper-diagonal canonical form

$$\Lambda = \begin{bmatrix} 0 & 1 & 0 & 0 & 0 \\ 0 & 0 & 1 & 0 & 0 \\ \vdots & \vdots & \vdots & \ddots & \vdots \\ 0 & 0 & 0 & 0 & 1 \\ 0 & 0 & 0 & 0 & 0 \end{bmatrix}, B = \begin{bmatrix} 0 \\ \vdots \\ 0 \\ 1 \end{bmatrix}, C = \begin{bmatrix} 1 \\ \vdots \\ 0 \\ 0 \end{bmatrix}^T, \tag{4}$$

where $s \in \mathbb{R}_+$ is the time variable, $\zeta(s) = (\zeta_1(s),\dots,\zeta_n(s))^T \in \mathbb{R}^n$ is the state vector, $u(s) \in \mathbb{R}$ is an input signal, available to the designer, $w(s)$ is the unknown disturbance, and $y_\zeta(s) \in \mathbb{R}$ is the only available measurement of the system.

Throughout, the disturbance $w(s)$ is assumed to be of class L_∞ and to possess an *a priori* known magnitude bound $L > 0$ such that

$$|w(s)| \leq L \text{ for all } s \in \mathbb{R}_+. \tag{5}$$

The reconstruction of the state vector for (3) over the available input/output information can be addressed by an estimator

$$\dot{\hat{\zeta}}(s) = \Lambda\hat{\zeta}(s) + Bu(s) + G(\tilde{\zeta}_1(s)), \tag{6}$$

where $\hat{\zeta}(s) = (\hat{\zeta}_1(s),\dots,\hat{\zeta}_n(s))^T \in \mathbb{R}^n$ is the estimator state initialized with $\hat{\zeta}^0 = \hat{\zeta}(0) \in \mathbb{R}^n$, the injection vector

$$G(\tilde{\zeta}_1(s)) = \Big(g_1(\tilde{\zeta}_1(s)),\dots,g_n(\tilde{\zeta}_1(s))\Big)^T \tag{7}$$

depends on the estimation output error

$$\tilde{\zeta}_1(s) = \zeta_1(s) - \hat{\zeta}_1(s) \in \mathbb{R}, \tag{8}$$

of the available measurement $y_\zeta(s) = \zeta_1(s)$. Estimator (6) is associated with the error equation

$$\dot{\tilde{\zeta}}(s) = \Lambda\tilde{\zeta}(s) + Bw(s) - G(\tilde{\zeta}_1(s)), \tag{9}$$

initialized at $\tilde{\zeta}^0 = \tilde{\zeta}(0) \in \mathbb{R}^n$, where $\tilde{\zeta}(s) = \zeta(s) - \hat{\zeta}(s) \in \mathbb{R}^n$ is the estimation error.

Following [11], let (7) be specified with the components

$$g_i(\tilde{\zeta}_1(s)) = k_i L^{\frac{i}{n}} \lceil \tilde{\zeta}_1(s) \rfloor^{\frac{n-i}{n}}, \quad i = 1,\dots,n \tag{10}$$

where L is the upper bound of the disturbance magnitude (5) and $k_1,\dots,k_n$ are design parameters. Then the origin $\tilde{\zeta} = 0$ of the observation error dynamics (9) is finite time stable under any admissible disturbance (5) provided that $k_1,\dots,k_n$ are properly chosen [3, Theorem 1]. With this in mind, estimator (6) represents a robust finite-time observer of system (3) in the upper-diagonal canonical form (4).

It should be noted that the last observer injection component

$$g_n(\tilde{\zeta}_1) = k_n L \lceil \tilde{\zeta}_1 \rfloor^0 = k_n L \operatorname{sign}\tilde{\zeta}_1$$

is a discontinuous function of the estimation error $\tilde{\zeta}_1$ which is why the meaning of the corresponding error dynamics is throughout viewed in the sense of Filippov [4].

2.2. Design extension: a case study

A linear system

$$\dot{x}(s) = Ax(s) + B\Big(u(s) + w(s)\Big),$$
$$y_x(s) = Cx(s) \tag{11}$$

with the same B, C as before and an arbitrary A such that the pair (A,C) is observable is well-known to be represented in the canonical form (3) by applying a certain linear non-singular state transformation. Hence, a finite-time observer for such a system (11) can be recast from the canonical form observer (6) by applying an appropriate state transformation.

The resulting finite-time observer is further specified for a particular case of (11) with the bi-diagonal matrix

$$A = \mathrm{diag}(\delta_i) + \Lambda, \tag{12}$$

composed of the upper-diagonal matrix Λ, governed by (4) and of a diagonal matrix with arbitrary entries $\delta_i,\ i = 1, \dots, n-1$ and $\delta_n = 0$. Such a system (11) is of interest as it constitutes a baseline system whose finite-time observer is recast into a prescribed-time observer of an arbitrary system in canonical form.

By inspection, the above pair (A, C) is observable with the observability matrix

$$\mathcal{O}_1 = \begin{bmatrix} C \\ CA \\ \vdots \\ CA^{n-1} \end{bmatrix} \tag{13}$$

of full rank n. Moreover, it is shown [13, Section 12.7] that a state transformation of the form

$$x(s) = Pz(s), \tag{14}$$

brings (11), (12) into the observer canonical form

$$\begin{aligned} \dot{z}(s) &= P^{-1}APz(s) + P^{-1}B\Big(u(s) + w(s)\Big), \\ y_z(s) &= CPz(s), \end{aligned} \tag{15}$$

with

$$P^{-1}B = B, \quad CP = C, \quad P^{-1}AP = \mathcal{A} \tag{16}$$

subject to

$$\mathcal{A} = \begin{bmatrix} -a_1 & 0 & \dots & 0 \\ -a_2 & 0 & \dots & 0 \\ \vdots & & \vdots & \\ -a_n & 0 & \dots & 0 \end{bmatrix} + \Lambda, \tag{17}$$

where $a_1, \dots, a_n$ are the coefficients of the characteristic equation

$$\det(\lambda I_n - A) = \lambda^n + a_1\lambda^{n-1} + \dots + a_{n-1}\lambda + a_n = 0 \tag{18}$$

of the original system (11), (12). Indeed, it is straightforward to verify that setting

$$\mathcal{O}_2 = \begin{bmatrix} C \\ C\mathcal{A} \\ \vdots \\ C\mathcal{A}^{n-1} \end{bmatrix} \tag{19}$$

and letting

$$P = \mathcal{O}_1^{-1}\mathcal{O}_2 \tag{20}$$

yield the transformed system (15) in the observer canonical form (16), (17).

Finite-time observer design for such a system in the observer canonical form (15)–(17) follows from that presented in Section 2.1 for the upper-diagonal form. The observer design for (15)–(17) is thus obtained in the form

$$\dot{\hat{z}}(s) = \mathcal{A}\hat{z}(s) + Bu(s) + F(\tilde{z}_1(s)), \tag{21}$$

where $\tilde{z}_1(s) = z_1(s) - \hat{z}_1(s)$ is the observation output error of system (15)–(17), (21),

$$F(\tilde{z}_1(s)) = (-a_1, -a_2, \dots, -a_n)^T\tilde{z}_1(s) + G(\tilde{z}_1(s)), \tag{22}$$

and the vector function G is determined by (7), (10). Then the error dynamics $\tilde{z}(s) = z(s) - \hat{z}(s)$ are governed by

$$\dot{\tilde{z}}(s) = \Lambda\tilde{z}(s) + Bw(s) - G(\tilde{z}_1(s)), \tag{23}$$

and along with (9), these dynamics are finite-time stable.

It is clear that a finite-time estimate $\hat{x}(s) = (\hat{x}_1(s), \dots, \hat{x}_n(s))^T$ of the original state variable (14) is readily reproduced by applying the state transformation $\hat{z}(s) = P^{-1}\hat{x}(s)$ to the observer dynamics (21). Indeed, employing (16) to conclude that

$$\tilde{z}_1 = C\tilde{z} = CP\tilde{z} = CPP^{-1}\tilde{x} = C\tilde{x} = \tilde{x}_1,$$

and setting $\tilde{x}_1(s) = x_1(s) - \hat{x}_1(s)$, the observer for system (11) in the bi-diagonal form (12) is obtained in the form

$$\begin{aligned} \dot{\hat{x}}(s) &= PP^{-1}APP^{-1}\hat{x}(s) + PP^{-1}Bu(s) \\ &\quad + PF\Big(CPP^{-1}\tilde{x}(s)\Big), \end{aligned} \tag{24}$$

which is further simplified to

$$\dot{\hat{x}}(s) = A\hat{x}(s) + Bu(s) + PF(\tilde{x}_1(s)). \tag{25}$$

Summarizing, the following result is in order.

Theorem 1. *Along with a linear perturbed system (11) in the bi-diagonal form (4), (12), consider its estimator (25), associated with the matrix factor (20) and the injection term (22), specified with (7), (10). Let the observer gains $k_1, \dots, k_n$ in (10) be chosen as in [3, Section IV] to ensure finite-time stability of (9) for any admissible disturbance (5). Then the observation error dynamics $\tilde{x}(s) = x(s) - \hat{x}(s)$ are finite-time stable regardless of whichever external disturbance (5) affects the underlying system (11).*

Proof. To begin with, let us note that $\tilde{x}(s) = P\tilde{z}(s)$ by construction. Since $\tilde{z}(s)$ is governed by (23), copying the observation error Eq. (9) for the upper-diagonal canonical system (3), (4), it remains to note that under conditions of Theorem 1, [3, Theorem 1] is applicable to (9). By applying [3, Theorem 1], (9) is concluded to be finite-time stable for any admissible disturbance (5). Thus, the observation error dynamics $\tilde{x}(s) = P\tilde{z}(s)$ in question are established to be finite-time stable, too, irrespectively of an admissible disturbance (5). This completes the proof of Theorem 1. □

For later use, the error dynamics

$$\frac{d}{ds}\tilde{x}(s) = A\tilde{x}(s) + Bw(t(s))e^{-s/T} - PF(\tilde{x}_1(s)), \tag{26}$$

are straightforwardly obtained from the state-observer Eqs. (11) and (25).

3. Prescribed-time observer design

In this section, the observer design is further developed for the system

$$\begin{aligned} \dot{\eta}(t) &= \Lambda\eta(t) + B\Big(u(t) + w(t)\Big), \\ y_\eta(t) &= C\eta(t) \end{aligned} \tag{27}$$

in the upper-diagonal form (4), running in the time variable $t \in \mathbb{R}_+$.

The design objective is to meet a prescribed upper bound $T > 0$ on the observer convergence time, which is independent of the initial states and admissible disturbances. For this purpose, the hybrid observer

$$\dot{\hat{\eta}}(t) = \Lambda\hat{\eta}(t) + Bu(t) + Q(\tilde{\eta}_1(t), t), \tag{28}$$

is involved with the state estimate $\hat{\eta}(t) = (\hat{\eta}_1(t), \dots, \hat{\eta}_n(t))^T$ and input injection $Q(\tilde{\eta}_1, t) = \Big(q_1(\tilde{\eta}_1, t), \dots, q_n(\tilde{\eta}_1, t)\Big)^T$, given by

$$Q(\tilde{\eta}_1, t) = \begin{cases} \mathcal{M}(t)PF(\mu_1^{n-1}(t)\tilde{\eta}_1), & \text{if } |\operatorname{sign}\tilde{\eta}_1| = 1, \\ G(\tilde{\eta}_1), & \text{otherwise.} \end{cases} \tag{29}$$

The time-varying injection term (29) depends on the output estimation error $\tilde{\eta}_1(t) = \eta_1(t) - \hat{\eta}_1(t)$, and it relies on P and F, governed by (20) and (22), respectively, and on the diagonal matrix

$$\mathcal{M}(t) = \mathrm{diag}\Big(\mu_1^{2-n}(t), \mu_1^{3-n}(t) \dots, \mu_1^{n-n}(t), \mu_1(t)\Big) \tag{30}$$

where

$$\mu_1(t) = \frac{T}{T-t}, \quad 0 \le t < T \tag{31}$$

is inherited from [17].

The hybrid observer (28)–(31) is composed of the finite-time stabilizing components (10) of the injection term $G(\tilde{\eta}_1(t)) : \mathbb{R} \to \mathbb{R}^n$, acting iff $|\operatorname{sign}\tilde{\eta}_1| \neq 1$, and its time-varying counterpart $\mathcal{M}(t)PF(\mu_1^{n-1}(t)\tilde{\eta}_1)$, confined to the set $\{\tilde{\eta} \in \mathbb{R}^n : |\operatorname{sign}\tilde{\eta}_1| = 1\}$. As shown in the stability proof below, the time-varying observer component $F(\mu_1^{n-1}(t)\tilde{\eta}_1)$, governed by (22) and tuned according to (7) and (10) with the gains $k_1, \dots, k_n$, declared by Theorem 1, enforces the observation error to reset to zero faster than in the prescribed time T. Right after that, it switches to the autonomous correction term $G(\tilde{\eta}_1(t))$ which keeps the observation error in the sliding mode that occurs in the origin $\tilde{\eta}_i = 0$ $i = 1, \dots, n$ of the error state space once $|\operatorname{sign}\tilde{\eta}_1| \neq 1$.

By inspection, the error dynamics are governed by

$$\dot{\tilde{\eta}}(t) = \Lambda\tilde{\eta}(t) + Bw(t) - Q(\tilde{\eta}_1(t), t). \tag{32}$$

Specifically, the time-varying observer substructure

$$\dot{\hat{\eta}}(t) = \Lambda\hat{\eta}(t) + Bu(t) + \mathcal{M}(t)PF(\mu_1^{n-1}(t)\tilde{\eta}_1), \tag{33}$$

is pre-composed in such a manner that the corresponding error dynamics

$$\dot{\tilde{\eta}}(t) = \Lambda\tilde{\eta}(t) + Bw(t) - \mathcal{M}(t)PF(\mu_1^{n-1}(t)\tilde{\eta}_1) \tag{34}$$

are deducible from the error dynamics (26). To make such a deduction it suffices to specify (12) with

$$\delta_i = \frac{n-i}{T}, \ \ i = 1, \dots, n-1$$

and to rewrite (26) in terms of the rescaled time variable

$$s(t) = -T\ln\left(\frac{T-t}{T}\right) : [0, T) \to [0, \infty) \tag{35}$$

and rescaled states

$$\tilde{x}_i(s(t)) = \mu_1^{n-i}(t)\tilde{\eta}_i(t), \ \ i = 1, \dots, n, \tag{36}$$

compactly represented in the vector form

$$\tilde{x}(s(t)) = \mu_1(t)\mathcal{M}^{-1}(t)\tilde{\eta}(t). \tag{37}$$

To validate the underlying relation (36) between the error dynamics (26) and (34) for any disturbance applied, the additive perturbation of (26) has deliberately been specified in the form

$$w(t(s))e^{-s/T} = \frac{w(t(s))}{\mu_1(t(s))}, \tag{38}$$

using the inverse time transformation

$$t(s) = T(1 - e^{-s/T}) : \mathbb{R}_+ \to [0, T) \tag{39}$$

to (35). Such a disturbance is clearly estimated

$$|w(t(s))e^{-s/T}| \le |w(t(s))| \le L$$

by the magnitude upperbound L inherited from (5).

By construction, the error dynamics (34) are settled to zero faster than T regardless of any initial conditions and any uniformly bounded disturbance (5). Indeed, the dynamics (26) was shown in Theorem 1 to vanish in a finite time instant

$$S_0(\tilde{x}^0, k_1, \dots, k_n, w)$$

which depends on the initial values $\tilde{x}^0 = \tilde{x}(0)$, on the properly chosen gains $\{k_i\}_{i=1}^n$, and on the applied disturbance (38). Hence, in the original time variable t, the error dynamics (34) vanish at $T_0(S_0) = T(1 - e^{-S_0/T}) < T$, i.e., before the time-varying gain (31) escapes to infinity at $t = T$. This is the main motivation of using the nonlinear observer instead of the linear prescribed-time observer [6], which faces the implementation problem for the infinite gain (31) when $t \to T$. In addition, the observer robustification over the infinite horizon is obtained.

It is clear that T_0 constitutes the switching time instant

$$T_0 = \inf\left\{t \in [0, T] : \operatorname{sign}\tilde{\eta}_1(t) \in (-1, 1)\right\} \tag{40}$$

and it is associated with the moment when the sliding mode occurs in the origin $\tilde{\eta}_i(t) = 0$ $i = 1, \dots, n$. By the equivalent control method [19], the sign function $\operatorname{sign}\tilde{\eta}_1(t)$ in (29) takes intermediate values within the interval $(-1, 1)$ in the origin $\tilde{\eta}_i(t) = 0$, $i = 1, \dots, n$ only because otherwise it takes an extremal value 1 or -1. Indeed, the observer dynamics (28), (29) cross the axis $\tilde{\eta}_1(t) = 0$ everywhere but the origin where the sliding mode of order n occurs. Since $\tilde{\eta}_i(t)$, $i = 2, \dots, n$ are not available to the designer, the only option of switching the observer structure is to automatically switch it online at the time instant (40) when the sliding mode starts.

The following result is thus established.

Theorem 2. *Under conditions of Theorem 1, consider system (27) in the upper-diagonal canonical form (4) and its observer (28)–(31), specified with (20), (22) and an arbitrarily small $T > 0$ independent of initial conditions and admissible disturbances. Then the error dynamics (32) are fixed-time stable with the convergence time $T_0 < T$ and with the bounded time-varying gain (31), applied at the initial stage $[0, T_0)$ only.*

Proof. By inspection, relation (36) between the error dynamics (26) and (34) is straightforwardly verified for $t \in [0, T_0)$. In other words, the system (26) represents the initial behavior of the observer error dynamics (34) for $t \in [0, T_0)$, expressed in the rescaled time (35) and state variables (36). Since the rescaled error dynamics (26) are finite-time stable by Theorem 1 regardless of whichever admissible disturbance affects the dynamics, it follows that the original error dynamics (34) are robustly finite-time stable, too, with the settling time $T_0 < T$.

Indeed, due to (36) where $\mu_1(t) \ge 1$ by its definition (31), one concludes that $\tilde{\eta}_i(t) = 0$, $i = 1, \dots, n$ at some $t = T_0(\tilde{\eta}^0, w, k_1, \dots, k_n) < T$ that depends on the initial values $\tilde{\eta}^0 = \tilde{\eta}(0)$, admissible disturbance $w(t)$, and observer gains $\{k_i\}_{i=1}^n$ taken as in [3, Section IV] to ensure finite-time stability of (9) under any disturbance (5). Moreover, (31) remains bounded because it is switched off after T_0.

Thus, at the time instant $t = T_0$, the observer error dynamics (32) switch the injection term to the correction term $G(\tilde{\eta}_1(t)) : \mathbb{R} \to \mathbb{R}^n$ which, by [3, Theorem 1], rejects admissible disturbances and keep the error states in the origin for all $t \ge T_0$. This completes the proof of Theorem 2. □

4. Illustrative example

The effectiveness of the observer (28)–(31) is further tested in a simulation study where system (27) is of the third order, i.e., $\eta(t) \in \mathbb{R}^3$ and the matrices in (4) are given by

$$\Lambda = \begin{bmatrix} 0 & 1 & 0 \\ 0 & 0 & 1 \\ 0 & 0 & 0 \end{bmatrix}, B = \begin{bmatrix} 0 \\ 0 \\ 1 \end{bmatrix}, C = \begin{bmatrix} 1 \\ 0 \\ 0 \end{bmatrix}^T. \tag{41}$$

The states of the model (27), (41), initiated at the origin $\eta(0) = 0 \in \mathbb{R}^3$ of the state space, are assumed to be enforced by

$$u(t) = a_u \sin(\omega_1^u t), \tag{42}$$

$$w(t) = a_w[\sin(\omega_1^w t) + \cos(\omega_2^w t)], \tag{43}$$

specified with the parameters

$$a_u = 10, \ \omega_1^u = 2\pi, \ a_w = 0.1, \ \omega_1^w = 2\pi, \ \omega_2^w = 4\pi. \tag{44}$$

Table 1
Observer data.

PT observer [6, Theorem 1]
Injection terms
$\gamma_1(t) = l_1 + (\frac{m+3}{T} - \tilde{p}_{21})\mu_1(t)$,
$\gamma_2(t) = l_2 + (\frac{m+4}{T}\tilde{p}_{21} - \tilde{p}_{31})\mu_1(t)^2 - \gamma_1(t)\tilde{p}_{21}\mu_1(t)$,
$\gamma_3(t) = l_3 + \frac{m+5}{T}\tilde{p}_{31}\mu_1(t)^3 - \gamma_1(t)\tilde{p}_{31}\mu_1(t)^2 - \gamma_2(t)\tilde{p}_{32}\mu_1(t)$,
$q_1(\tilde{\eta}_1, t) = \gamma_1\tilde{\eta}_1(t)$, $q_2(\tilde{\eta}_1, t) = \gamma_2\tilde{\eta}_1(t)$, $q_3(\tilde{\eta}_1, t) = \gamma_3\tilde{\eta}_1(t)$,
$\mathcal{Q}(\tilde{\eta}_1, t) = [q_1(\tilde{\eta}_1, t), q_2(\tilde{\eta}_1, t), q_3(\tilde{\eta}_1, t)]^T$.
Parameters
$\tilde{p}_{21} = -2\frac{m+3}{T}$, $\tilde{p}_{31} = \frac{(m+3)(m+4)}{T^2}$, $\tilde{p}_{32} = -\frac{m+3}{T}$,
$T = 1.001$, $m = 1$, $l_1 = 3$, $l_2 = 8$, $l_3 = 4$.
FT observer [12, Theorem 2]
Injection terms
$q_1(\tilde{\eta}_1) = \theta\kappa_1(\lceil\tilde{\eta}_1\rfloor^{\alpha} + \lceil\tilde{\eta}_1\rfloor^{\beta})$,
$q_2(\tilde{\eta}_1) = \theta^2\kappa_2(\lceil\tilde{\eta}_1\rfloor^{2\alpha-1} + \lceil\tilde{\eta}_1\rfloor^{2\beta-1})$,
$q_3(\tilde{\eta}_1) = \theta^3\kappa_3(\lceil\tilde{\eta}_1\rfloor^{3\alpha-2} + \lceil\tilde{\eta}_1\rfloor^{3\beta-2})$,
$\mathcal{Q}(\tilde{\eta}_1, t) = [q_1(\tilde{\eta}_1), q_2(\tilde{\eta}_1), q_3(\tilde{\eta}_1)]^T$,
Parameters
$\alpha = 0.8$, $\beta = 1.2$, $\theta = 40$, $\kappa_1 = 3$, $\kappa_2 = 3$, $\kappa_3 = 1$.

Clearly,

$$|w(t)| \le 2a_w \text{ for all } t \in \mathbb{R}_+, \tag{45}$$

and the disturbance magnitude is therefore upper estimated by $L = 0.2$.

In the simulation runs, the observer (28)–(31) of model (27) was initialized at $\hat{\eta}_1(0) = \hat{\eta}_2(0) = \hat{\eta}_3(0) = 1$, and for adding practical values, it was tested in the presence of measurement noise $\psi(\cdot)$ in the observation channel, modelled as

$$y_\eta(t) = \eta_1(t) + \psi(t), \tag{46}$$

where

$$\psi(t) = 10^{-6}\sin(10^4 t). \tag{47}$$

The resulting measurement (46) is then substituted into the observer injection term (29) for $\eta_1(t)$. Along with this, the observer is specified with the prescribed time $T = 1$ s and the parameters $k_1 = 3.45$, $k_2 = 5.65$, $k_3 = 1.1$, $L = 5$ chosen as in [3, Section V.B].

The simulations were conducted using the Euler forward integration method with the integration step 1×10^{-5} s.

Fig. 1 shows that the observation error escapes to zero faster than the prescribed time $T = 1$ s, in the presence of the measurement noise $\psi(t)$ and disturbance $w(t)$.

The injection term (29), used in the proposed observer (28)–(31), is depicted in Fig. 2, to illustrate its uniform boundedness on the entire simulation time interval, i.e., before and after the prescribed time T.

4.1. Comparative study

For the sake of comparison, prescribed- and fixed-time observers, recently introduced in the literature, are compared with the hybrid observer (28)–(31) designed for (27), (41) in Section 4. The former, proposed in [6, Theorem 1], is further referred to as *PT observer*, and the latter, inherited from [12, Theorem 2], is further referred to as *FT observer*. For ease of reference, the prescribed-time observer (28)–(31) with finite gains is subsequently abbreviated as *PTFG observer*.

Both, the PT and FT observers, as well as the PTFG observer (28)–(31) are tested to estimate the unperturbed system (27), (41) with $w(t) \equiv 0$ when it is driven by the known input (42), (44) and the measurement noise (47) is present in the observation channel (46).

The injection observer terms, designed in [6, Theorem 1] and in [12, Theorem 2], are given in Table 1 with the accompanying parameters, used in the simulations. The parameters of the PTFG observer injection terms remains the same as before.

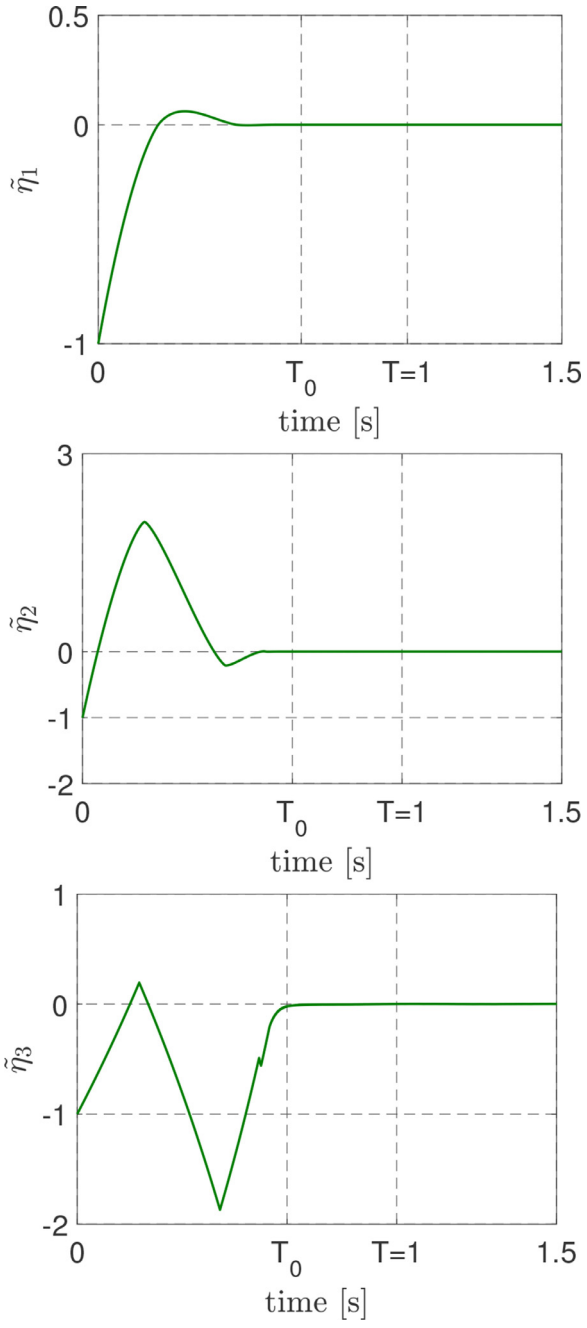

Fig. 1. Time responses of the observation errors with the prescribed convergence time bound $T = 1$ s.

4.1.1. PT and PTFG observer comparison

Recall that the PT observer deals with infinitely large gains $\frac{T^m}{(T-t)^m}$, $m = 1, 2, 3$, $t \in [0, T)$, escaping to infinity as the time variable t approaches the prescribed time T and resulting in numerical precision limitations [6, Section II-A]. This is in contrast to the developed observer (28)–(31), operating with finite time-varying gains on the infinite horizon (rather than on the prescribed-time interval $[0, T)$) and yielding the exact robust state estimate not only by the prescribed time instant T but also for all $t \ge T$.

Due to the above observations regarding the PT observer, a fair comparison of the observers is confined to the prescribed-time interval $[0, T)$ where the PT observer works adequately. To mitigate the implementation problem for the PT observer with infinitely large gains, the prescribed convergence time T is slightly extended

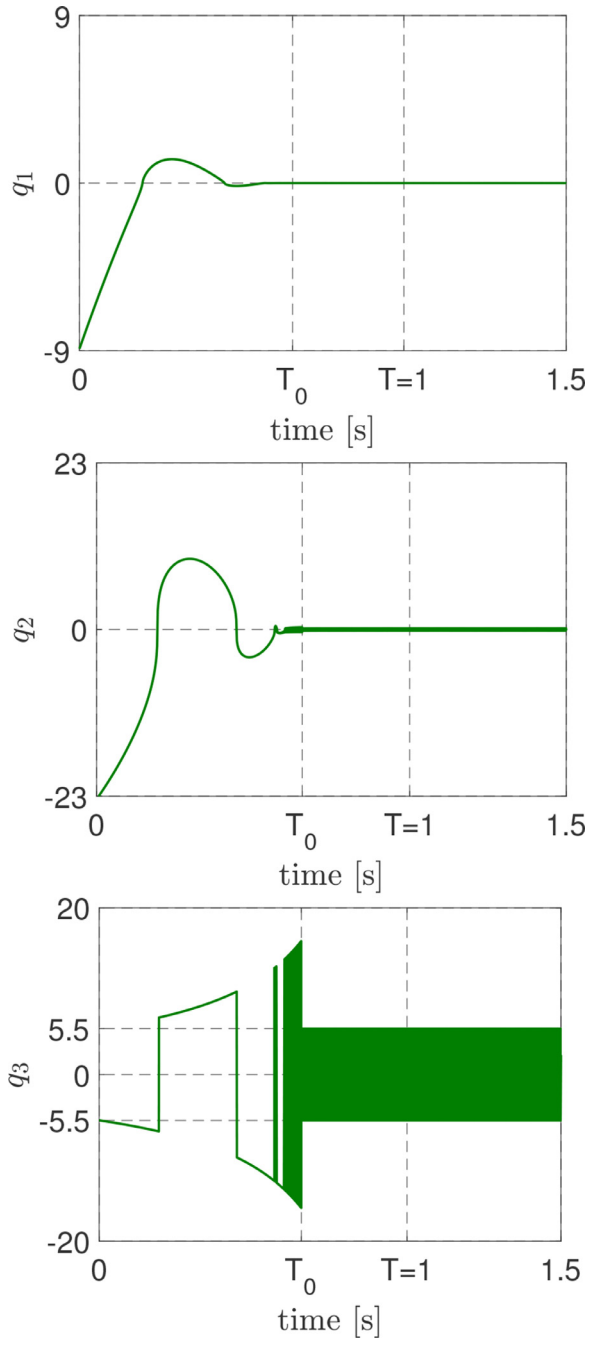

Fig. 2. Time responses of the injection components.

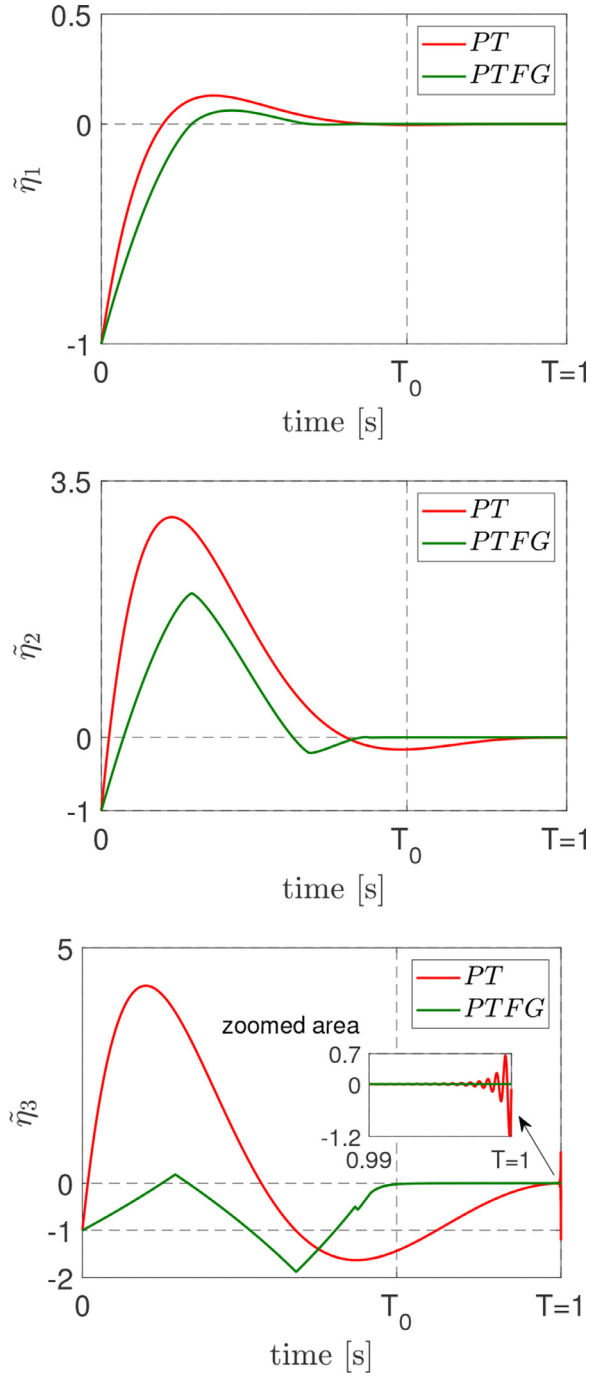

Fig. 3. Comparative simulations: time responses of the PT and PTFG observation errors.

to a larger value as recommended in [6, Section II-A]. In the simulations of the PT observer, the prescribed time is therefore set to $T = 1.001$ s thereby sacrificing the estimation error which is now guaranteed to converge to within some neighborhood of the origin only.

Fig. 3 depicts the estimation errors of the PT and PTFG observers. A harmful effect of the measurement noise is seen for the PT observer, producing that the estimation error $\tilde{\eta}_3(t)$, diverges near the prescribed time T when the low magnitude noise is magnified by an infinitely large observer gain. Such an undesired effect is however not present for the PTFG observer.

The injection terms (29), used in the proposed observer (28)–(31), together with those of the PT observer given in Table 1, are depicted in Fig. 4. As seen, the injection terms of the PT observer drastically grow near the prescribed time $T = 1$ s. Meanwhile the injection terms (29) of the PTFG observer remains uniformly bounded.

4.1.2. FT and PTFG observer comparison

The FT observer [12], with injection terms and parameters in Table 1, designed for system (27), (41), yields an observation error dynamics $\tilde{\eta}(t)$ whose settling time function is bounded according to [12, Theorem 2]

$$T_{FT}(\tilde{\eta}^0) \leq \frac{4}{\theta}\left(\frac{1}{1-\alpha} + \frac{1}{\beta - 1}\right), \tag{48}$$

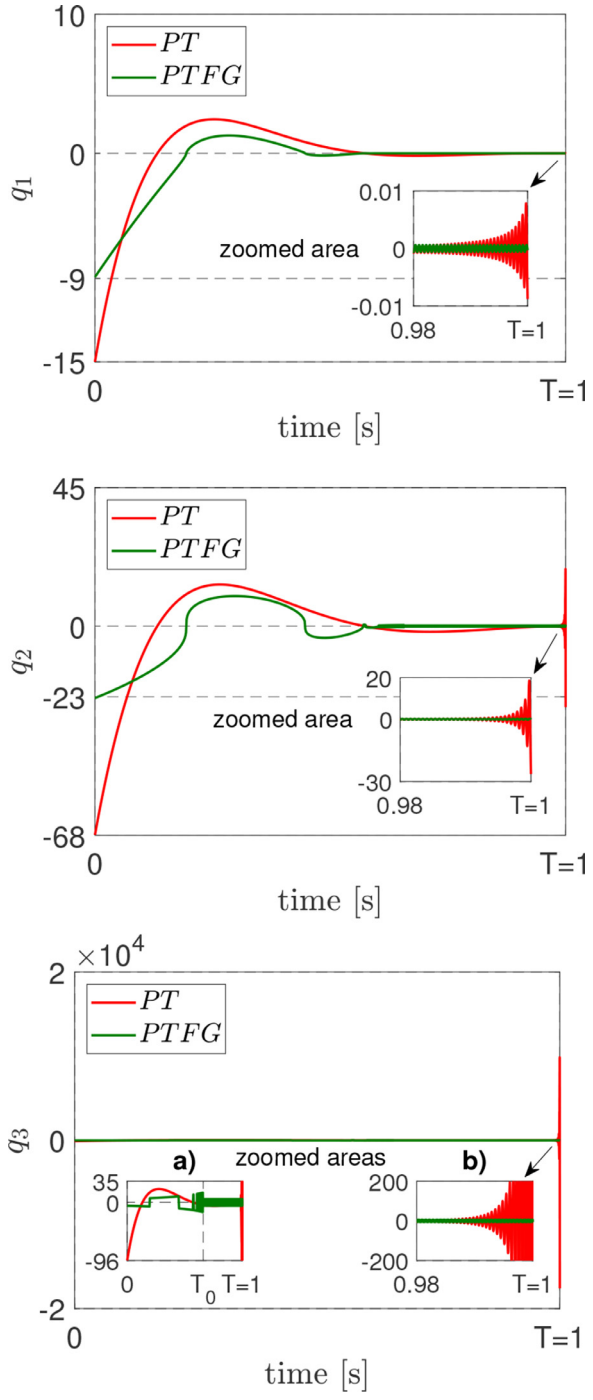

Fig. 4. Comparative simulations: time responses of the PT and PTFG injection terms.

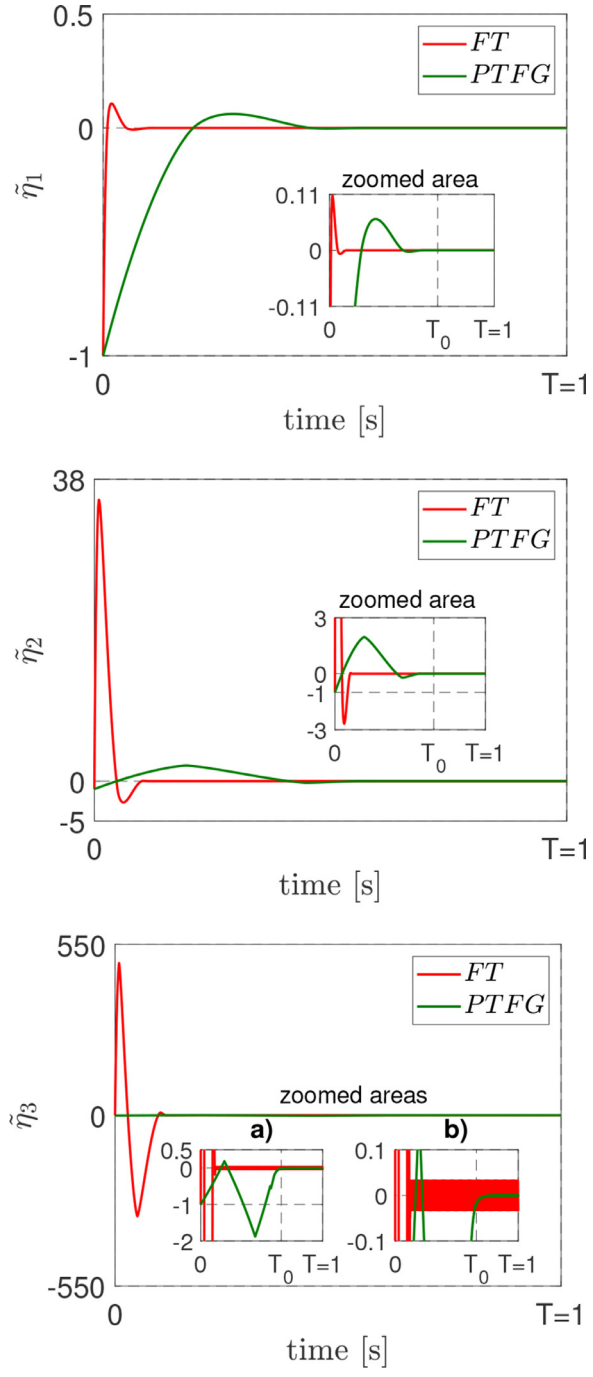

Fig. 5. Comparative simulations: time responses of the FT and PTFG observation errors.

regardless of the initial conditions $\tilde{\eta}^0(t) = \tilde{\eta}(0)$ of the observation error dynamics. Thus, under required parameter restrictions $\theta > 1$, $\alpha \in (1-\epsilon, 1)$, $\beta \in (1, 1+\epsilon)$ and $\epsilon > 0$ small enough, it is possible to *a priori* find an upper bound on the right-hand side of (48). Indeed, by taking the parameters of the FT observer as in Table 1, the settling time function (48) is upper bounded as $T_{FT}(\tilde{\eta}^0) \leq T$, where $T = 1$ s is the prescribed time for the proposed observer (28)–(31). Therefore, the observation error dynamics $\tilde{\eta}(t)$ of the FT observer is expected to vanish in a time no longer than $T = 1$ s.

The fixed-time convergence of the FT observer with the settling time function (48), upper bounded by $T = 1$ s, is corroborated in Fig. 5 where the observation errors are settled into the origin before $T = 1$ s. It should be noted however that the observation error transient response of the FT observer reaches bigger values than those of the PTFG observer. Besides, as clearly seen from the observation error $\tilde{\eta}_3(t)$ in the zoomed area b) of Fig. 5, the magnitude of the chattering is significantly bigger in the FT observer than in the PTFG observer.

The injection terms (29), used in the proposed observer (28)–(31), are depicted in Fig. 6 along with those of the FT observer given in Table 1. Considerably higher values are achieved by the initial time response of the injection terms of the FT observer compared to those of the PTFG observer. Higher chattering values are

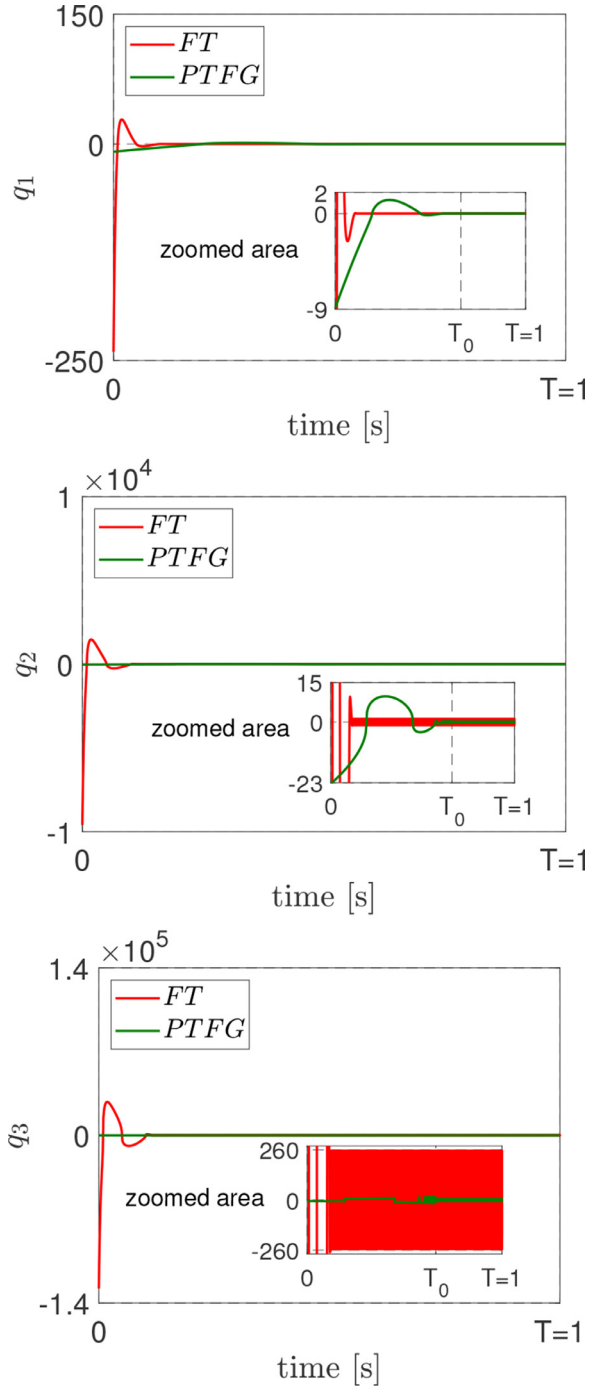

Fig. 6. Comparative simulations: time responses of the FT and PTFG injection terms.

also concluded for the injection terms of the FT observer vs. the injection terms of the PTFG observer.

The influence of the tuning parameter θ in the FT observer is clearly seen from Figs. 5 and 6. Being set as in Table 1, it results in the upper bound $T = 1$ s of the settling time function (48). However, besides the highest observation error transient response and injection terms values, it also yields an overestimated value of the settling time function of the observation error $\tilde{\eta}(t)$, which is approximately found from the simulation results to be 0.125 s. Hence, a higher sensitivity to low magnitude additive noise is experienced by the FT observer when compared with the PTFG observer.

5. Conclusions

Non-autonomous fixed-time observer design is proposed for an arbitrary-order normal-form system with a prescribed upper bound $T > 0$ on the observer convergence time. Similar to the original prescribed-time observer design [6], the proposed one is based on a time scaling, explicitly parameterized with T, and on a specific state transformation, recasting a fixed-time stable observer (rather than a Luenberger observer) for having the desired convergence rate.

The resulting observer gets a bonus of operating with uniformly bounded time-varying gains over the entire infinite horizon, and it is therefore straightforwardly implementable in a similar manner to its finite-time progenitor, reviewed in Section 2. This is in contrast to [6], facing infinitely large time-varying gains as $t \to T$ and thus manifesting the high-gain challenge for the observer implementation.

Good observer performance is illustrated in a numerical study of a perturbed triple integrator, operating under matched uniformly bounded disturbances and measurement noise. In comparison with the prescribed- and fixed-time observers of [6] and [12], the developed observer is particularly shown to possess lower sensitivity to low magnitude with high frequency noise added to the measurement channel. Extension of the present development to prescribed-time output feedback stabilization with uniformly bounded time-varying gains is among challenging problems calling for further investigation.

Declaration of Competing Interest

The authors Ramón I. Verdés Kairuz, Yury Orlov, and Luis T. Aguilar of the paper Robust Observer Design with Prescribed Settling Time Bound and Finite Varying Gains declare that they have no known competing financial interests or personal relationships that could have appeared to influence the work reported in this paper.

References

[1] R. Aldana-López, D. Gómez-Gutiérrez, M.A. Trujillo, M. Navarro-Gutiérrez, J. Ruiz-León, H.M. Becerra, A predefined-time first-order exact differentiator based on time-varying gains, Int. J. Robust Nonlinear Control 31 (11) (2021) 5510–5522, doi:10.1002/rnc.5536.
[2] Y. Chitour, R. Ushirobira, H. Bouhemou, Stabilization for a perturbed chain of integrators in prescribed time, SIAM J. Control Optim. 58 (2) (2020) 1022–1048, doi:10.1137/19M1285937.
[3] E. Cruz-Zavala, J.A. Moreno, Levant's arbitrary-order exact differentiator: a Lyapunov approach, IEEE Trans. Autom. Control 64 (7) (2019) 3034–3039, doi:10.1109/TAC.2018.2874721.
[4] A.F. Filippov, Differential Equations with Discontinuous Righthand Sides, Kluwer Academic Publisher, 1988.
[5] D. Gómez-Gutiérrez, On the design of nonautonomous fixed-time controllers with a predefined upper bound of the settling time, Int. J. Robust Nonlinear Control 30 (10) (2020) 3871–3885, doi:10.1002/rnc.4976.
[6] J. Holloway, M. Krstic, Prescribed-time observers for linear systems in observer canonical form, IEEE Trans. Autom. Control 64 (9) (2019a) 3905–3912, doi:10.1109/TAC.2018.2890751.
[7] J. Holloway, M. Krstic, Prescribed-time output feedback for linear systems in controllable canonical form, Automatica 107 (2019b) 77–85, doi:10.1016/j.automatica.2019.05.027.
[8] H.K. Khalil, High-Gain Observers in Nonlinear Feedback Control, SIAM, 2017.
[9] P. Krishnamurthy, F. Khorrami, M. Krstic, A dynamic high-gain design for prescribed-time regulation of nonlinear systems, Automatica 115 (2020) 108860, doi:10.1016/j.automatica.2020.108860.
[10] P. Krishnamurthy, F. Khorrami, M. Krstic, Adaptive output-feedback stabilization in prescribed time for nonlinear systems with unknown parameters coupled with unmeasured states, Int. J. Adapt. Control Signal Process. 35 (2021) 184–202, doi:10.1002/acs.3193.
[11] A. Levant, Higher-order sliding modes, differentiation and output-feedback control, Int. J. Control 76 (9/10) (2003) 924–941, doi:10.1080/0020717031000099029.
[12] T. Menard, E. Moulay, W. Perruquetti, Fixed-time observer with simple gains for uncertain systems, Automatica 81 (2017) 438–446, doi:10.1016/j.automatica.2017.04.009.
[13] N.S. Nise, Control Systems Engineering, John Wiley & Sons, 2007.

[14] Y. Orlov, Finite time stability and robust control synthesis of uncertain switched systems, SIAM J. Control Optim. 43 (4) (2005) 1253–1271, doi:10.1137/S0363012903425593.
[15] Y. Orlov, R.I. Verdés Kairuz, L.T. Aguilar, Prescribed-time robust differentiator design using finite varying gains, IEEE Control Syst. Lett. 6 (2021) 620–625, doi:10.1109/LCSYS.2021.3084134.
[16] A. Polyakov, Nonlinear feedback design for fixed-time stabilization of linear control systems, IEEE Trans. Autom. Control 57 (8) (2012) 2106–2110, doi:10.1109/TAC.2011.2179869.
[17] Y. Song, Y. Wang, J. Holloway, M. Krstic, Time-varying feedback for regulation of normal-form nonlinear systems in prescribed finite time, Automatica 83 (2017) 243–251, doi:10.1016/j.automatica.2017.06.008.
[18] D. Tran, T. Yucelen, Finite-time control of perturbed dynamical systems based on a generalized time transformation approach, Syst. Control Lett. 136 (2020) 104605, doi:10.1016/j.sysconle.2019.104605.
[19] V. Utkin, Sliding Modes in Control and Optimization, Springer–Verlag, Berlin, Heidelberg, 1992.
[20] R.I. Verdés Kairuz, Y. Orlov, L.T. Aguilar, Prescribed-time stabilization of controllable planar systems using switched state feedback, IEEE Control Syst. Lett. 5 (6) (2020) 2048–2053, doi:10.1109/LCSYS.2020.3046682.
[21] H. Ye, Y. Song, Prescribed-time control of uncertain strict-feedback-like systems, Int. J. Robust Nonlinear Control 31 (11) (2021) 5281–5297, doi:10.1002/rnc.5541.
[22] B. Zhou, Finite-time stabilization of linear systems by bounded linear time-varying feedback, Automatica 113 (2020) 108760, doi:10.1016/j.automatica.2019.108760.
[23] B. Zhou, Y. Shi, Prescribed-time stabilization of a class of nonlinear systems by linear time-varying feedback, IEEE Trans. Autom. Control 66 (12) (2021) 6123–6130, doi:10.1109/TAC.2021.3061645.